**Proceedings of the IASTED International Conference**
**POWER AND ENERGY SYSTEMS**
**May 13-15, 2002, Marina del Rey, California, USA**

# Dynamic Models for Interaction between Wind Turbines and Power Systems

Poul Sørensen and Anca D. Hansen
Risø National Laboratory
Wind Energy Department
P.O.Box 49
DK-4000 Roskilde, Denmark

Frede Blaabjerg
Aalborg University
Institute of Energy Technology
Pontoppidanstræde 101
DK-9220 Aalborg East, Denmark

John Bech
NEG-Micon Control Systems
Italiensvej 1-5
DK-8450 Hammel, Denmark

## ABSTRACT

Because of the fast development of wind energy, concentrated in areas with good wind resources, wind energy has become an increased role in the power system. This paper describes a model used to simulate the power quality of a wind farm. The ability of the model to predict power quality is validated, using definitions from the newly released IEC 61400-21 final draft international standard (FDIS) for power quality of grid connected wind turbines.

## KEY WORDS:

Wind turbines, power quality, simulation models.

## 1. INTRODUCTION

The utilization of wind energy has developed very fast during the last two decades. In the same period, the wind turbine technology has matured with a reduction of the production costs from 1.20 DKK/kWh to less than 0.30 DKK/kWh [1]. The optimization of the mechanical and aeroelastic design of the wind turbines together with the industrialization of the production process combined with the up-scaling of the average wind turbine size are the main reasons for this price reduction.

The fast wind energy development has been concentrated in areas with good wind resources, which are essential for the feasibility of the wind energy installations. Another factor, which has strongly affected the development, is the subsidy policy of the national governments. The different subsidy policies are also a major reason for the concentration of the wind energy development.

The fast development in some areas has given rise to an increased influence of the wind energy on the power systems in these areas. The most important concern of the wind energy development from the utilities point of view has been the influence on the voltage quality, on the power system operation and control and on the stability in the event of grid faults.

So far, the largest part of the wind energy development has been based on single wind turbines, clusters or wind farms connected to the distribution system. For this type of installations, first of all the voltage quality at the consumers connected near to wind turbine installations has been a concern. This has lead to a number of national standards and requirements for grid connection of wind turbines to the distribution system through the last decades.

Internationally, IEC issued an FDIS (Final Draft International Standard) IEC 61400-21 [2] for measurement and assessment of power quality of grid connected wind turbines in December 2001. The IEC standard defines a common set of wind turbine power quality measures to be used in the national requirements.

Today, wind energy units with hundreds of MW installed capacity are planned and developed in Denmark, USA and other countries. These units have sizes comparable to power plant blocks, and must be connected to the transmission systems.

The large size of the units makes the systems more dependent on the reliability of the wind farms, which brings focus to the stability of the wind farms in the event of grid faults and to the ability of the wind farms to participate in the system control of voltage of frequency. The focus on grid fault stability is caused by the wish to prevent the loss of a large wind farm due to a grid fault.

In Denmark, the transmission system operators have issued specifications for connecting wind farms to the transmission network [3]. These specifications involve requirements on the grid fault stability and controllability of the wind farms besides the requirements to power quality. Also in Germany, the operators are making new requirements to the grid fault stability of wind turbines.

The present large scale of wind energy in some power systems increases the need to predict the influence of further wind energy development in these systems. This has caused an increased interest for the use of simulation tools to predict the interaction between wind turbines and power systems.

The required simulation models for the different issues have many things in common, but also some differences e.g. in the time scale, which is in focus. Dynamic models for prediction of the influence of wind turbines on the power quality and on the voltage and frequency control of the power systems are typically focusing on time scales from milliseconds to minutes, whereas models for simulation of grid fault stability focus on faster time scales from microseconds to a few seconds.

The present paper focus on a model developed to predict the power quality of the wind farm in Hagesholm, Denmark. The Hagesholm wind farm consits of six 2MW NM-72/2000 wind turbines from NEG-Micon. The power control of the NM-72/2000 machines is performed by active stall control of the blade angles.

The models have been developed in the dedicated power system simulation tool DIgSILENT. With this tool, models for traditional load flow and transient simulations are combined with RMS based models useful for the relevant time scales for power quality. Simulated power quality characteristics of a single wind turbine and of two wind turbines operating simultaneously are compared to measurements.

## 2. IEC 61400-21 CHARACTERISTICS

IEC 61400-21 defines a set of power quality characteristics for wind turbines, and specifies the methods to measure these characteristics in a power quality test of a single wind turbine. The power characteristics are based on power and currents rather than voltages. Thus, the power quality test is a type test with applicability for grid connection of the same type of wind turbines on other grids than the grid where the wind turbine was tested.

IEC 61400-21 defines characteristics for continuous operation of the wind turbine as well as for switching operations. This chapter will limit the presentation of the characteristics for continuous operation only.

### 2.1. Maximum power

IEC 61400-21 specifies maximum power with two different average times, a fast averaging with 200 ms and a slow averaging with 1 minute. The corresponding maximum values are denoted $P_{0.2}$ and $P_{60}$, respectively. The idea is to use $P_{0.2}$ to relay protection design, whereas $P_{60}$ can be used for load flow analyses of voltage profiles and thermal loading of the system components.

To estimate the maximum power of a wind farm consisting of $N_{\mathrm{wt}}$ wind turbines, IEC 61400-21 recommends to calculate the maximum 60 second power $P_{60\Sigma}$ of the wind farm according to

$$P_{60\Sigma} = \sum_{i=1}^{N_{wt}} P_{60i} \qquad (1)$$

where $P_{60i}$ is the maximum power of the $i^{\mathrm{th}}$ wind turbine. This recommendation is based on the assumption that the fluctuations in the 60 s average power are identical for all wind turbines, i.e. the power variations are fully correlated, and consequently the maximum value appear at the same time at all wind turbines. This is a conservative assumption, but also very convenient.

For the 0.2 s average power, IEC 61400-21 recommends a summation that assumes that these fast fluctuations are uncorrelated. The maximum 0.2s average power of the wind farm is calculated as

$$P_{0.2\Sigma} = \sum_{i=1}^{N_{wt}} P_{ni} + \sqrt{\sum_{i=1}^{N_{wt}} \left(P_{0.2i} - P_{ni}\right)^2} \qquad (2)$$

where $P_{0.2i}$ is the 200 ms maximum power of the $i^{\mathrm{th}}$ wind turbine and $P_{ni}$ is the rated power of the $i^{\mathrm{th}}$ wind turbine.

In a wind farm with 64 wind turbines of the same type, each with a 0.2 ms maximum power 40 % above rated power, the 0.2 ms maximum power of the wind farm will be estimated to 5% above the rated power of the wind farm according to ( 2 ) . This is a substantial reduction compare to a worst case assumption that the wind farm maximum would be the same 40 % above rated as for the individual wind turbines.

If we assume that the 60 s maximum power of the individual wind turbines are 10 % above rated power, then the estimated wind farm maximum is also 10 % above the rated wind farm power of the wind farm according to ( 1 ). In this case, the estimated wind farm 0.2 ms maximum power is less than the estimated 60 s maximum power, which is statistically impossible. The 0.2 s average maximum power will always be greater than the 60 s average maximum power. A more consistent method would be to use $P_{60i}$ instead of $P_{ni}$ in ( 2 ). Then only the fluctuations faster than 60 s are assumed to be uncorrelated, and $P_{0.2\Sigma}$ would always be greater than $P_{60\Sigma}$.

### 2.2. Reactive power

The reactive power which must be measured according to IEC 61400-21 is the steady state or average value in each 10 % bin of the active power, i.e. for 10 %, 20 % etc. of the rated power. The fluctuations in reactive power are included by specification of the reactive power at maximum power rather than the maximum (or minimum) reactive power, because these are the values which are useful for load flow analyses.

## 2.3. Voltage fluctuations and flicker

IEC 61400-21 specifies a flicker coefficient $c(\psi)$ to characterize the flicker emission from a wind turbine. The flicker coefficient is a normalized measure for the flicker emission from the wind turbine on a grid with the network impedance phase angle $\psi$, giving the flicker short term emission $P_{st}$ and long term emission $P_{lt}$ according to

$$P_{st} = P_{lt} = c(\psi) \cdot \frac{S_n}{S_k} \qquad (3)$$

where $S_n$ is the rated apparent power of the wind turbine and $S_k$ is the short circuit power of the gird.

The flicker coefficient strongly depends on the network impedance angle, because active power fluctuations contribute strongest to flicker emission at lower network impedance angles, while reactive power fluctuations contribute strongest to flicker emission at higher network impedance angles. For angles in between, the flicker emission from a wind turbine is often smaller than for higher as well as lower angles, because many wind turbines consume reactive power, which normally implies that $\partial Q/\partial P<0$. Still, for wind turbines with power converters, e.g. for connection of the rotors of double fed induction generators, the reactive power production / consumption can be controlled.

IEC 61400-21 requires the flicker coefficients to be specified for four network impedance angles: 30 deg, 50 deg, 70 deg and 85 deg.

# 3. MODEL DESCRIPTION

## 3.1. Grid model

The grid model is shown in Figure 1. The grid is built on standard component models from the DIgSILENT library.

Each (n) of the six wind turbines is connected to its own 10 kV bus WTn_10kV. The figure shows how the wind farm is connected to the substation in two groups. A backup line is also installed between the ends of the two lines.

The substation is modelled with double busbars and transformers with automatic tap changers. The 50 kV grid is simply modelled by a Thevenin equivalent. This is a fair approximation for power quality studies, because the wind farm has relatively little influence on the power quality of the 50 kV grid, which is strong compared to the installed wind power capacity.

A number of load feeders are also connected to the substation in Grevinge. As a tentative solution, these loads are modelled by a single, general load directly connected to the 10 kV busbar of the substation

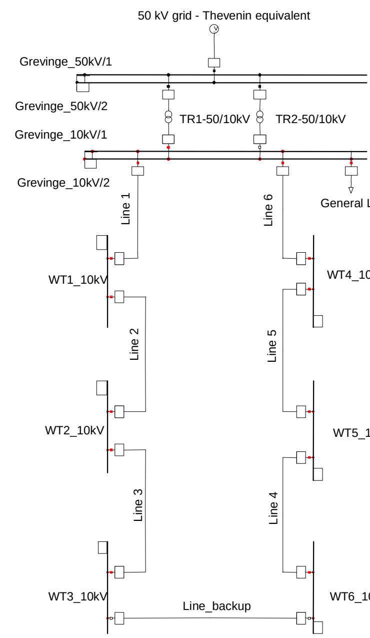


**Figure 1: Grid model for the connection of Hagesholm wind farm.**

## 3.2. Wind turbine model

A dynamic wind turbine model is connected to each of the wind turbine terminals WTn_10kV in Figure 1. Each of the wind turbines are modelled individually, providing a realistic model for the dynamics of the wind farm, where the wind turbines can operate with different wind speed and mechanical fluctuations, coupled through the grid.

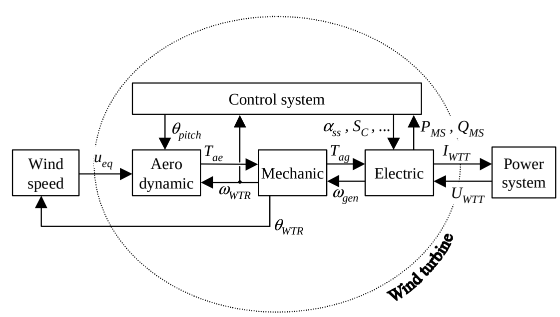


**Figure 2: Wind turbine model with interface to power system (grid) model and wind speed model.**

An overview of the model of an individual wind turbine is shown in Figure 2. It includes an electric part, a mechanical part and an aerodynamic part. The electric part provides the interface to the grid as the currents $I_{WTT}$ and voltages $U_{WTT}$ on the wind turbine terminals, while the aerodynamic part is feeded by an equivalent wind speed $u_{eq}$ described in section 3.3. Note that the wind model uses the turbine rotor position $\theta_{WTR}$ from the mechanical part of the wind turbine model, which will also be explained in section 3.3.The wind turbine model includes a control system block. Inputs to the control system block are the active and the reactive power $P_{MS}$ and $Q_{MS}$ measured at the main switch, and the turbine rotor speed $\omega_{WTR}$. The outputs from the control block are the pitch angle $\theta_{pitch}$ for the aerodynamic model, and a number of control signals for the electric model, including soft starter firing angle $\alpha_{ss}$ and capacitor switch signals $S_C$.

### 3.2.1. Electrical model

The electric part of the wind turbine model is shown in Figure 3. It includes induction generator, softstarter, capacitor banks for reactive power compensation and the step-up transformer. The transformer is placed in the hub at the top of the tower, and the 10 kV cable through the tower is included in the model.

$P_{MS}$ and $Q_{MS}$ in Figure 2 are taken from the low voltage side of the step-up transformer, corresponding to where the wind turbine control system measures voltage and current on the main switch.

The capacitor bank consists of 10 steps, which are controlled independently. The control system model sends signals to the contacts, to close or open the individual capacitors, based on the measured $Q_{MS}$.

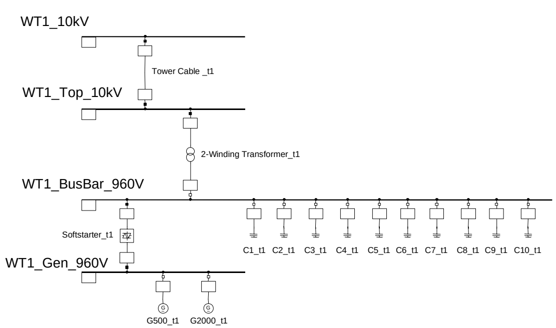


**Figure 3: Model of the electric part of the wind turbine.**

The softstarter is controlled by the firing angle. The control system model calculates this firing angle like the control system of the real wind turbine. This is implemented in DIgSILENT, based on the dynamic simulation language.

Two different generators are connected to the 960 kV busbar in Figure 3. This corresponds to the two sets of windings in the real generator with 4 and 6 poles.

### 3.2.2. Mechanical model

The mechanical model of the wind turbine is shown in Figure 4. It is essentially a two mass model connected by a flexible shaft characterised by a stiffness $k_{ms}$ and a damping $c_{ms}$. Moreover, an ideal gear with the exchange ratio *1:f* is included.

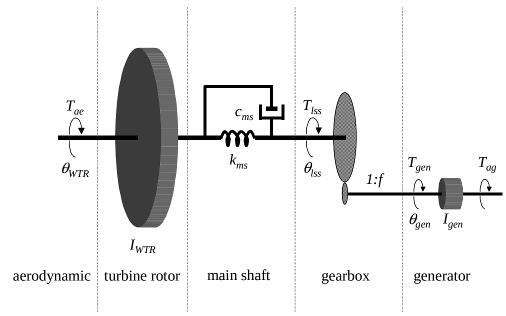


**Figure 4: Model of the mechanical part of the wind turbine.**

The masses used in this model correspond to a large turbine rotor inertia $I_{WTR}$ representing the blades and hub, and a small inertia $I_{gen}$ representing the induction generator. The generator inertia is actually included in the generator model, specified as an inertia time constant.

The stiffness and damping components are modelled on the low speed shaft, but flexibility in the gear and on the high speed shaft can also be included here, if they are corrected for the gear ratio.

### 3.2.3. Aerodynamic model

The aerodynamic model is based on tables with the aerodynamic efficiency $C_p$ defined according to

$$P_{ae} = \frac{1}{2} \rho \, A \, u_{eq}^{\;3} \, C_p \tag{4}$$

where $P_{ae}$ is the aerodynamic power, $A$ is the swept rotor area and $\rho$ is the air density. $C_p = C_p(\lambda, \theta_{pitch})$ depends on the blade pitch angle $\theta_{pitch}$ and the blade tip speed ratio $\lambda$ defined according to

$$\lambda = \frac{\omega_{WTR} \cdot R}{v_{eq}} \tag{5}$$

where $\omega_{WTR}$ is the rotor speed and $R$ is the radius of the rotor.

Traditional $C_p$ models are based on steady state aerodynamics, which underestimates the power fluctuations in the stall region at high wind speeds. Since the power quality characteristics normally depend decisively on the power fluctuations at high wind speeds, the present model includes the dynamic stall effects. The applied model for dynamic stall is based on Øye's dynamic stall model [4]. A more detailed description of the model is given in [5].

### 3.3. Wind model

Variations in the wind speed in space and time is the excitation to wind turbines and wind farms, which generates power fluctuations during continuous operation. Therefore, the wind model is essential to obtain realistic simulations of power fluctuations during continuous operation.

The wind model used for the present power quality simulations is described in details by Sørensen et.al. [6]. It includes the (park scale) coherence of the wind speeds at different wind turbines as well as the effects of the wind variations in the rotor plane.

The park scale coherence is included, because it ensures realistic fluctuations in the sum of the power from each wind turbine, which is important for prediction of the maximum power output from the wind farm. It is a stochastic model, which simulates wind speeds at the wind turbines, taking into account the coherence between wind speeds at different wind turbines.

The variations in the rotor plane are included because they cause most of the flicker emission during continuous operation [7]. It includes the deterministic effect from tower shadow as well as stochastic effect from turbulence variations in the rotor disk. As the blades rotate in the rotor plane, the spatial wind speed variations appear as time variations of the wind speeds acting on the blades.

## 4. POWER QUALITY VERIFICATION

For the power quality verification, six 10 minute measurements have been selected around 9 m/s and two around 15 m/s. For each of the eight measurements, a corresponding simulation with the same wind characteristics (mean wind speed and turbulence intensity) has been performed.

### 4.1. Maximum power

Figure 5 shows the maximum values of the measured and simulated 200 ms average power. The simulated maximum power of the time series with approximately 9 m/s mean wind speed are slightly greater than the measured maximum power. The average difference between simulated and measured maximum is 31 kW or 2 % of the measured maximum, which is a very small difference, taking into account the uncertainty of comparing only six 10 minute time series. Concerning the maximum values of the two time series with approximately 15 m/s mean wind speed, the uncertainty is even greater, but the average difference between simulated and measured maximums is –307 kW or 13 % of the measured maximum.

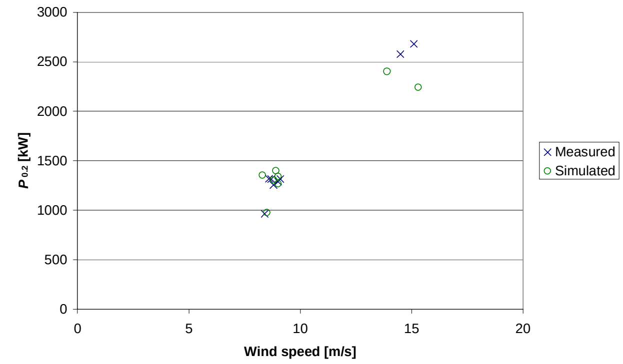


**Figure 5: Measured and simulated maximum values of 200 ms average power of wind turbine 1 in the selected eight 10 minute time series.**

Figure 6 shows the maximum values of the 200 ms average power sum. The average difference between the simulated and measured maximum of the sum power of the time series with approximately 9 m/s mean wind speed is 43 kW, i.e. slightly greater simulated than the measured maximum power like for wind turbine 1 alone. The average difference between the simulated and measured maximum values of the two time series with approximately 15 m/s mean wind speed is –385 kW.

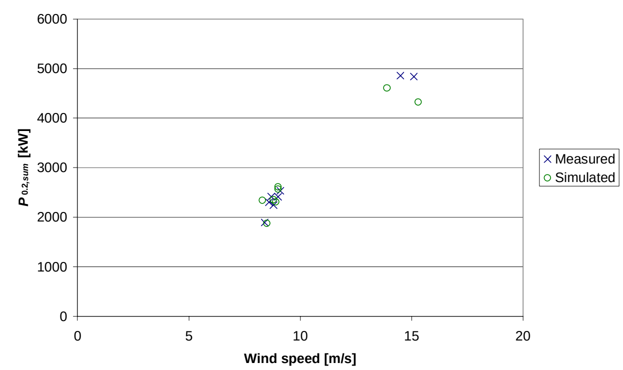


**Figure 6: Measured and simulated values of 200 ms average of summed power of wind turbine 1 and wind turbine 2 in the selected eight 10 minute time series.**

The maximum 60 s average power have also been compared. This comparison also shows quite good agreement. The detailed results can be found in [5].

### 4.2. Reactive power

The 10 minutes mean values of the reactive power vs. active power of the selected six time series with mean wind speed 9 m/s are shown in Figure 7. We see a very good agreement between the scatter of measured and simulated reactive power for the six runs. The average difference between simulated and measured reactive power is only –6 kvar.

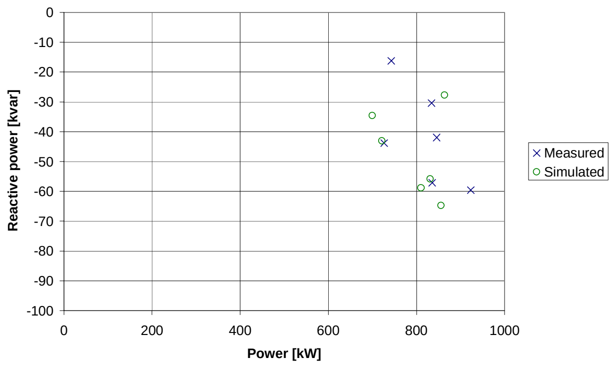


**Figure 7. 10 min mean values of reactive power vs. active power.**

The steady state reactive power appears to be very well simulated using the six runs at 9 m/s.

### 4.3. Flicker

Figure 8 shows the measured and simulated flicker coefficients of the selected eight time series for 30 deg network impedance angles. As with maximum power, we see a very good agreement at 9 m/s, while the underestimated fluctuations at 15 m/s causes lower simulated flicker emission than measured flicker emission.

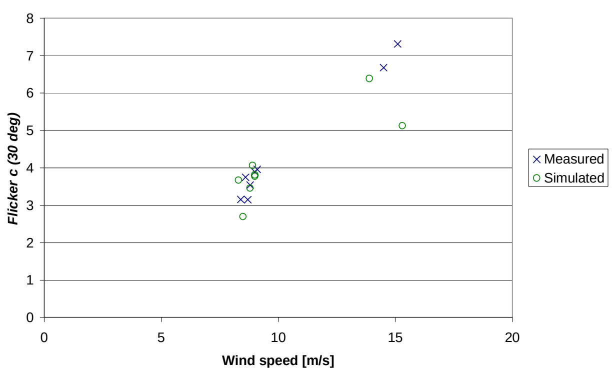


**Figure 8. Measured and simulated flicker coefficients for continuous operation of wind turbine 1. Network impedance angle 30 deg.**

## 5. CONCLUSION

The paper has presented a model for simulation of the power quality of a wind farm. The simulation results show a very good agreement between measured and simulated power quality at wind speeds about 9 m/s. Comparisons have also been performed at 15 m/s, where the agreement seems to be not quite as good.

Appropriate wind models are essential to obtain realistic simulation results. The wind models must include the coherence between the wind speeds at different wind turbines to account for the smoothing effect of the power fluctuations in a wind farm compared to the power fluctuations of the individual wind turbines. In order to account for the fast, flicker generating fluctuations, the wind model must also include modeling of the spatial wind speed variations in the swept area.

Dynamic stall modeling is essential to simulate the power fluctuations in the wind turbine stall region, i.e. at about 15 m/s for (active) stall controlled wind turbines. This effect is included in the present model.

## 6. ACKNOWLEDGEMENT

The Danish Energy Agency is acknowledged for the funding of this work in the contracts ENS-1363/00-0003 and ENS-1363/01-0013. Besides, a special thanks is given to North-West Sealand Energy Supply Company, NVE, who has provided grid data and assisted at the power quality measurements.

## REFERENCES

[1] *IEA Wind Energy Annual Report 2000*. (National Renewable Energy Institute, Golden, CO, 2001).

[2] IEC 61400-21. *Wind turbine generator systems – Measurement and assessment of power quality of grid connected wind turbines* (IEC, Geneva, Switzerland, 2001).

[3] *Specifications for connecting wind farms to the transmission network*, (Eltra, DK, 2000).

[4] S.Øye, Dynamic stall - simulated as time lag of separation, *Proceedings of the 4th IEA Symposium on the Aerodynamics of Wind Turbines* (1991).

[5] P. Sørensen, A.D.Hansen, L.Janosi,J.Bech & B. Bak-Jensen, *Simulation of interaction between wind farm and power system*. (Risø-R-1281(EN), DK, 2001).

[6] P. Sørensen, A.D. Hansen & P.A.C. Rosas, Wind models for prediction of power fluctuations from wind farms. *5. Asia-Pacific conference on wind engineering, Kyoto (JP), 21-24 Oct 2001. J. Wind Eng.(89)*, 2001, 9-18.

[7] P. Sørensen, A.D. Hansen, L. Janosi, B. Bak-Jensen, F. Blaabjerg & J. Bech, Simulation of wind farm interaction with grid. *Wind energy for the new millennium. Proceedings. 2001 European wind energy conference and exhibition (EWEC '01)*, Copenhagen, DK, 2001, 1003-1006.